

TUM/T39-00-09
ECT-00-006
hep-ph/0007293

Axial U(1) dynamics in η and η' photoproduction ^{*}

Steven D. Bass^[ab], Stefan Wetzel^[a] and Wolfram Weise^[a]

^a *Physik Department, Technische Universität München,
D-85747 Garching, Germany*

^b *ECT*, Strada delle Tabarelle 286, I-38050 Villazzano, Trento, Italy*

Abstract

We discuss the sensitivity of η and η' photoproduction near threshold to the gluonic OZI breaking parameters in the $U_A(1)$ -extended effective chiral Lagrangian for low-energy QCD. Our coupled-channels analysis hints at a strong correlation between the gluon-induced contributions to the η' mass and the low-energy $pp \rightarrow pp\eta'$ reaction and the near-threshold behaviour of the $\gamma p \rightarrow \eta p$ cross-section.

^{*}Work supported in part by BMBF and DFG.

1 Introduction

Gluonic degrees of freedom play an important role in the physics of the flavour-singlet $J^P = 1^+$ channel [1] through the QCD axial anomaly [2]. The most famous example is the $U_A(1)$ problem: the masses of the η and η' mesons are much greater than the values they would have if these mesons were pure Goldstone bosons associated with spontaneously broken chiral symmetry [3, 4]. This extra mass is induced by non-perturbative gluon dynamics [5, 6, 7, 8] and the axial anomaly [9, 10]. In this paper we study the effect of gluons in axial $U(1)$ dynamics on η and η' photoproduction close to threshold. The η photoproduction process has been extensively studied at MAMI [12]. An important feature of the low-energy $\gamma p \rightarrow \eta p$ reaction is the prominent role of the S-wave resonance $N^*(1535)$. The $\gamma p \rightarrow \eta' p$ reaction is presently being studied at ELSA [13] and Jefferson Laboratory [14]. The first, and trivial, observation is that the thresholds themselves are sensitive to OZI violation through the gluonic component to the meson masses. More challenging is to understand the role of the axial anomaly and non-perturbative glue in the structure of the $N^*(1535)$ resonance which couples strongly to the η , and the shape of the η and η' photoproduction cross-sections with increasing energy. Our aim here is to study the sensitivity of the S-wave cross-sections to the gluonic OZI parameters in the $U_A(1)$ -extended effective chiral Lagrangian [15, 16, 17] for low-energy QCD. We illustrate the importance of $U_A(1)$ dynamics to these processes.

The role of gluonic degrees of freedom and OZI violation in the η' -nucleon system has previously been investigated through the flavour-singlet Goldberger-Treiman relation [18, 19] and the low-energy $pp \rightarrow pp\eta'$ reaction [17]. We frame our photoproduction discussion in the context this previous work. The flavour-singlet Goldberger-Treiman relation connects the flavour-singlet axial-charge $g_A^{(0)}$ measured in polarised deep inelastic scattering with the η' -nucleon coupling constant $g_{\eta'NN}$. Working in the chiral limit it reads

$$Mg_A^{(0)} = \sqrt{\frac{3}{2}}F_0 \left(g_{\eta'NN} - g_{QNN} \right) \quad (1)$$

where $g_{\eta'NN}$ is the η' -nucleon coupling constant and g_{QNN} is an OZI violating coupling which measures the one particle irreducible coupling of the topological charge density $Q = \frac{\alpha_s}{4\pi}G\tilde{G}$ to the nucleon. In Eq.(1) M is the nucleon mass and F_0 ($\sim 0.1\text{GeV}$) renormalises [17] the flavour-singlet decay constant. The coupling constant g_{QNN} is, in part, related [18] to the amount of spin carried by polarised gluons in a polarised proton. The large mass of the η' and the small value of $g_A^{(0)}$

$$g_A^{(0)}|_{\text{pDIS}} = 0.2 - 0.35 \quad (2)$$

extracted from deep inelastic scattering [20, 21, 22] (about a 50% OZI suppression) point to substantial violations of the OZI rule in the flavour-singlet $J^P = 1^+$ channel. A large positive $g_{QNN} \sim 2.45$ is one possible explanation of the small value of $g_A^{(0)}|_{\text{pDIS}}$.

Working with the $U_A(1)$ -extended chiral Lagrangian for low-energy QCD one finds a gluon-induced contact interaction in the $pp \rightarrow pp\eta'$ reaction close to threshold [17]:

$$\mathcal{L}_{\text{contact}} = -\frac{i}{F_0^2} g_{QNN} \tilde{m}_{\eta_0}^2 \mathcal{C} \eta_0 \left(\bar{p} \gamma_5 p \right) \left(\bar{p} p \right) \quad (3)$$

Here \tilde{m}_{η_0} is the gluonic contribution to the mass of the singlet 0^- boson and \mathcal{C} is a second OZI violating coupling which also features in $\eta'N$ scattering. The physical interpretation of the contact term (3) is a “short distance” ($\sim 0.2\text{fm}$) interaction where glue is excited in the interaction region of the proton-proton collision and then evolves to become an η' in the final state. This gluonic contribution to the cross-section for $pp \rightarrow pp\eta'$ is extra to the contributions associated with meson exchange models [23, 24, 25]. There is no reason, a priori, to expect it to be small. Following the earlier work at SATURNE [26] there is presently a vigorous experimental programme to investigate η and η' production near threshold in pN collisions at CELSIUS [27] and COSY [28]. Theoretical and experimental studies of $g_A^{(0)}$ and the η' -nucleon system may offer new insight into the role of gluons in chiral dynamics.

In this paper we investigate the S-wave contribution to η and η' photoproduction. The theoretical tools are the meson-baryon “potentials” derived from the low-energy $SU(3)_L \otimes SU(3)_R \otimes U_A(1)$ chiral effective Lagrangian together with the Lippmann-Schwinger equation. We extend the coupled channels analysis of Kaiser, Waas and Weise [29] to include η - η' mixing plus the coupling of axial $U_A(1)$ degrees of freedom to the nucleon. The $SU(3)$ coupled channels approach has been shown [29, 30, 31] to dynamically generate S-wave nucleon resonance contributions to low-energy hadron scattering as quasi-bound meson-baryon states.

We find that a positive value of the gluonic coupling \mathcal{C} in Eq.(3) generates an attractive contribution to the η -nucleon and η' -nucleon potentials in the Lippmann-Schwinger equation. It may, in part, contribute to the sharp rise in the η photoproduction cross-section very close to threshold. The $\gamma p \rightarrow \eta' p$ cross-section rises with increasing positive \mathcal{C} and is suppressed for negative \mathcal{C} . Our calculations suggest that in the gedanken world where OZI is preserved the $S_{11}(1535)$ contribution to $\sigma(\gamma p \rightarrow \eta p)$ would split into two resonance-like structures as we reduce the gluonic contribution to the η (and η') mass. The heavier structure is associated with a $K\Sigma$ quasi-bound state; the second, close to threshold, involves strong coupling to the $K\Lambda$ and ηN channels through the $K\Lambda \leftrightarrow \eta N$ potential.

The structure of the paper is as follows. In Section 2 we outline the coupled channels calculation. In Section 3 we briefly review the low-energy effective Lagrangian for η -nucleon and η' -nucleon interactions with emphasis on the sources of possible OZI violation. In Section 4 we present the numerical results. Finally, in Section 5, we make our conclusions.

2 Coupled channels calculation

The Lippmann-Schwinger equation for the T-matrix connecting in- and out- going channels j and i is

$$T_{ij} = V_{ij} + \sum_n \frac{2}{\pi} \int_0^\infty dl \frac{l^2}{k_n^2 - l^2 + i0} \left(\frac{\alpha_n^2 + k_n^2}{\alpha_n^2 + l^2} \right)^2 V_{in} T_{nj} \quad (4)$$

This is illustrated in Fig.1. We sum over two-particle intermediate states labelled by an index n which runs from 1 to 7 and refers to

$$|n\rangle = |\pi N\rangle^{(1/2)}, |\eta N\rangle^{(1/2)}, |K\Lambda\rangle^{(1/2)}, |K\Sigma\rangle^{(1/2)}, |N\eta'\rangle^{(1/2)}, |\pi N\rangle^{(3/2)}, |K\Sigma\rangle^{(3/2)}, \quad (5)$$

where the superscript labels isospin. These states are connected through the energy-dependent driving terms (which we call “potentials” for convenience) [29]:

$$V_{ij} = \frac{\sqrt{M_i M_j}}{4\pi^2 F_\pi^2 \sqrt{s}} C_{ij}, \quad (6)$$

where C_{ij} are the relative coupling strengths (up to a factor $-F_\pi^{-2}$ where F_π is the pion decay constant). These C_{ij} for S-wave amplitudes are calculated from the $U_A(1)$ -extended low-energy chiral Lagrangian – see Eqs.(19), (23) and (25) below – up to $O(p^2)$ in the meson momentum. Working to $O(p^2)$ means at most quadratic in the meson centre of mass energy $E_i = \frac{s - M_i^2 + m_i^2}{\sqrt{s}}$ where \sqrt{s} is the total centre of mass energy, and M_i and m_i are the baryon and meson masses in channel i . The potential V_{ij} is iterated to all orders using the Lippmann-Schwinger equation (4). In (4) l denotes the relative momentum of the off-shell meson-baryon pair in the intermediate state n and $k_n = \sqrt{E_n^2 - m_n^2}$ is the on-shell relative momentum. The form-factor $\left(\frac{\alpha_n^2 + k_n^2}{\alpha_n^2 + l^2} \right)^2$ renders the l -integral in (4) convergent. Here the α_n denotes a finite-range parameter for each channel n which has to fit to experimental data. One expects α_n to lie in the range 0.5 – 1 GeV for the SU(3) sector. The Lippmann-Schwinger equation (4) for the multi-channel T-matrix T_{ij} is solved by simple matrix inversion

$$T = \left(1 - V \cdot G \right)^{-1} V \quad (7)$$

where G is the diagonal matrix

$$G_n = \frac{2}{\pi} \int_0^\infty dl \frac{l^2}{k_n^2 - l^2 + i0} \left(\frac{\alpha_n^2 + k_n^2}{\alpha_n^2 + l^2} \right)^2 = \frac{k_n^2}{2\alpha_n} - \frac{\alpha_n}{2} - ik_n \quad (8)$$

The resulting multi-channel S-matrix is $S_{ij} = \delta_{ij} - 2i\sqrt{k_i k_j} T_{ij}$ with the total S-wave cross-section for the process $j \rightarrow i$,

$$\sigma_{ij} = 4\pi \frac{k_i}{k_j} |T_{ij}|^2. \quad (9)$$

This approach has been used to successfully describe a variety of meson-baryon and photoproduction processes in [29, 30, 31].

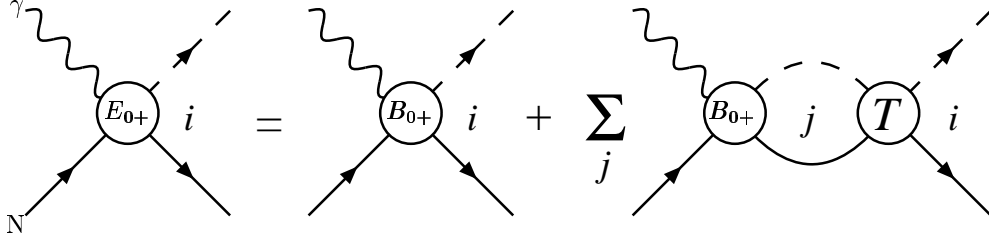


Figure 1: *Graphical representation of the Lippmann-Schwinger equation for S-wave meson photoproduction. The full, broken and wavy lines represent baryons, mesons and the photon, respectively.*

3 The low-energy effective Lagrangian

We work with the low-energy effective Lagrangian derived in [15, 16, 17]. Here we outline the features which are essential for our coupled channels calculation focussing on the key sources of possible OZI violation. Throughout, we shall work to second order in the meson fields and the meson momentum p_μ .

3.1 Glue and the η and η' masses

Starting in the meson sector, the $U_A(1)$ -extended low-energy effective Lagrangian [15, 16] is

$$\begin{aligned} \mathcal{L}_m = & \frac{F_\pi^2}{4} \text{Tr}(\partial^\mu U \partial_\mu U^\dagger) + \frac{F_\pi^2}{4} \text{Tr} \left[\chi_0 (U + U^\dagger) \right] \\ & + \frac{1}{2} i Q \text{Tr} \left[\log U - \log U^\dagger \right] + \frac{3}{\tilde{m}_{\eta_0}^2 F_0^2} Q^2. \end{aligned} \quad (10)$$

Here

$$U = \exp \left(i \frac{\phi}{F_\pi} + i \sqrt{\frac{2}{3}} \frac{\eta_0}{F_0} \right) \quad (11)$$

is the unitary meson matrix where $\phi = \sum_k \phi_k \lambda_k$ with ϕ_k denotes the octet of would-be Goldstone bosons (π, K, η_8) associated with spontaneous chiral $SU(3)_L \otimes SU(3)_R$ breaking, η_0 is the singlet boson, and λ_k are the Gell-Mann matrices; $\chi_0 = \text{diag}[m_\pi^2, m_\pi^2, (2m_K^2 - m_\pi^2)]$ is the meson mass matrix. The pion decay constant $F_\pi = 92.4 \text{ MeV}$; F_0 renormalises the flavour-singlet decay constant.

The $U_A(1)$ gluonic potential involving the topological charge density $Q = \frac{\alpha_s}{4\pi} G_{\mu\nu} \tilde{G}^{\mu\nu}$ generates the gluonic contribution to the η and η' masses. The gluonic term Q is treated as a background field with no kinetic term. It may be eliminated through its equation of motion

$$\frac{1}{2} i Q \text{Tr} \left[\log U - \log U^\dagger \right] + \frac{3}{\tilde{m}_{\eta_0}^2 F_0^2} Q^2 \mapsto -\frac{1}{2} \tilde{m}_{\eta_0}^2 \eta_0^2 \quad (12)$$

in Eq.(10) making the mass term clear. The $U_A(1)$ potential is also constructed to reproduce the axial anomaly [9, 10] in the divergence of the gauge-invariantly

renormalised flavour-singlet axial-vector current in the effective theory, viz.

$$\partial^\mu J_{\mu 5} = \sum_{k=1}^f 2i \left[m_k \bar{q}_k \gamma_5 q_k \right]_{GI} + N_f \left[\frac{\alpha_s}{4\pi} G_{\mu\nu} \tilde{G}^{\mu\nu} \right]_{GI}^{\mu^2} \quad (13)$$

where

$$J_{\mu 5} = \left[\bar{u} \gamma_\mu \gamma_5 u + \bar{d} \gamma_\mu \gamma_5 d + \bar{s} \gamma_\mu \gamma_5 s \right]_{GI}^{\mu^2}. \quad (14)$$

Here $N_f = 3$ is the number of light flavours, the subscript GI denotes gauge invariant renormalisation and the superscript μ^2 denotes the renormalisation scale. The Adler-Bardeen theorem [32] is used to constrain the possible $U_A(1)$ breaking terms in the effective Lagrangian.

After Q is eliminated from the effective Lagrangian via (12), we expand \mathcal{L}_m to $\mathcal{O}(p^2)$ in momentum keeping finite quark masses and obtain:

$$\begin{aligned} \mathcal{L}_m = & \sum_k \frac{1}{2} \partial^\mu \phi_k \partial_\mu \phi_k + \frac{1}{2} \partial_\mu \eta_0 \partial^\mu \eta_0 \left(\frac{F_\pi}{F_0} \right)^2 - \frac{1}{2} \tilde{m}_{\eta_0}^2 \eta_0^2 \\ & - \frac{1}{2} m_\pi^2 \left(2\pi^+ \pi^- + \pi_0^2 \right) - m_K^2 \left(K^+ K^- + K^0 \bar{K}^0 \right) - \frac{1}{2} \left(\frac{4}{3} m_K^2 - \frac{1}{3} m_\pi^2 \right) \eta_8^2 \\ & - \frac{1}{2} \left(\frac{2}{3} m_K^2 + \frac{1}{3} m_\pi^2 \right) \left(\frac{F_\pi}{F_0} \right)^2 \eta_0^2 + \frac{4}{3\sqrt{2}} \left(m_K^2 - m_\pi^2 \right) \left(\frac{F_\pi}{F_0} \right) \eta_8 \eta_0 \end{aligned} \quad (15)$$

In the chiral limit, $\chi_0 = 0$, gluons contribute a finite mass

$$m_{\eta_0}^2 = \tilde{m}_{\eta_0}^2 \left(\frac{F_0}{F_\pi} \right)^2 \quad (16)$$

to the singlet η_0 .

For finite quark masses η - η' mixing occurs. For simplicity we work in the one mixing angle scheme [33]:

$$\begin{aligned} |\eta\rangle &= \cos \theta |\eta_8\rangle - \sin \theta |\eta_0\rangle \\ |\eta'\rangle &= \sin \theta |\eta_8\rangle + \cos \theta |\eta_0\rangle \end{aligned} \quad (17)$$

The physical value of θ is taken as -18 degrees [33, 34]. The masses of the physical η and η' mesons are found by diagonalising the (η_8, η_0) mass matrix which follows from Eq.(15).

The value of F_0 is usually determined from the decay rate for $\eta' \rightarrow 2\gamma$. In QCD one finds the relation [35]

$$\frac{2\alpha}{\pi} = \sqrt{\frac{3}{2}} F_0 \left(g_{\eta'\gamma\gamma} - g_{Q\gamma\gamma} \right) \quad (18)$$

The observed decay rate [36] is consistent [33] with the OZI prediction for $g_{\eta'\gamma\gamma}$ if F_0 and $g_{Q\gamma\gamma}$ take their OZI values: $F_0 \simeq F_\pi$ and $g_{Q\gamma\gamma} = 0$. Motivated by this observation it is common to take $F_0 \simeq F_\pi$. In this paper we shall allow F_π/F_0 to vary between 0.8 and 1.25.

3.2 OZI violation and the η' -baryon interaction

The low-energy effective Lagrangian (10) is readily extended to include η -nucleon and η' -nucleon coupling. Working to $O(p)$ in the meson momentum the chiral Lagrangian for meson-baryon coupling is

$$\begin{aligned}\mathcal{L}_{\text{mB}} = & \text{Tr } \bar{B}(i\gamma_\mu D^\mu - M_0)B & (19) \\ & + F \text{Tr}(\bar{B}\gamma_\mu\gamma_5[a^\mu, B]_-) + D \text{Tr}(\bar{B}\gamma_\mu\gamma_5\{a^\mu, B\}_+) \\ & + \frac{i}{3}K \text{Tr}(\bar{B}\gamma_\mu\gamma_5B) \text{Tr}(U^\dagger\partial^\mu U) - \frac{\mathcal{G}_{QNN}}{2M_0}\partial^\mu Q \text{Tr}(\bar{B}\gamma_\mu\gamma_5B) + \frac{\mathcal{C}}{F_0^4}Q^2 \text{Tr}(\bar{B}B)\end{aligned}$$

Here

$$B = \begin{pmatrix} \frac{1}{\sqrt{2}}\Sigma^0 + \frac{1}{\sqrt{6}}\Lambda & \Sigma^+ & p \\ \Sigma^- & -\frac{1}{\sqrt{2}}\Sigma^0 + \frac{1}{\sqrt{6}}\Lambda & n \\ \Xi^- & \Xi^0 & -\frac{2}{\sqrt{6}}\Lambda \end{pmatrix} \quad (20)$$

denotes the baryon octet and M_0 denotes the baryon mass in the chiral limit. In Eq.(19)

$$D_\mu B = \partial_\mu B - ie\mathcal{A}_\mu[e_q, B] + \frac{1}{8F_\pi^2}[[\phi, \partial_\mu\phi], B] + \dots \quad (21)$$

is the chiral covariant derivative where $e_q = \text{diag}[\frac{2}{3}, -\frac{1}{3}, -\frac{1}{3}]$ is the quark charge matrix and \mathcal{A}_μ is the photon field; a_μ is the axial-vector current operator

$$a_\mu = -\frac{1}{2F_\pi}\partial_\mu\phi - \frac{1}{2F_0}\sqrt{\frac{2}{3}}\partial_\mu\eta_0 + \frac{ie}{2F_\pi}\mathcal{A}_\mu[e_q, \phi] + \dots \quad (22)$$

The chiral covariant derivative in (21) is independent of the singlet boson η_0 . The SU(3) couplings are $F = 0.459 \pm 0.008$ and $D = 0.798 \pm 0.008$ [37]. The $U_A(1)$ coupling K is dimensionless and the two gluonic couplings \mathcal{G}_{QNN} and \mathcal{C} both have mass dimension -3. In general, one may expect OZI violation wherever a coupling involving the Q -field occurs.

We shall work consistently to $O(p^2)$. This means that we include the chiral corrections to the baryon masses:

$$\mathcal{L}_{\text{mass}}^{(2)} = b_D \text{Tr}(\bar{B}\{\chi_+, B\}_+) + b_F \text{Tr}(\bar{B}[\chi_+, B]_-) + b_0 \text{Tr}(\bar{B}B) \text{Tr}\chi_+ \quad (23)$$

where

$$\begin{aligned}\chi_+ &= \left(\xi^\dagger\chi_0\xi^\dagger + \xi\chi_0\xi\right) & (24) \\ &= 2\chi_0 + 2\left(-\frac{1}{8F_\pi^2}\{\phi\{\phi, \chi_0\}_+\}_+ - \frac{1}{3F_0^2}\chi_0\eta_0^2 - \frac{1}{2}\sqrt{\frac{2}{3}}\frac{1}{F_\pi F_0}\eta_0\{\phi, \chi_0\}_+ + \dots\right)\end{aligned}$$

and $\xi = U^{\frac{1}{2}}$. We also include the heavy-baryon terms [29]

$$\mathcal{L}_{\text{HB}}^{(2)} = 2d_D \text{Tr}(\bar{B}\{(v \cdot a)^2, B\}) + 2d_F \text{Tr}(\bar{B}[(v \cdot a)^2, B]) \quad (25)$$

$$\begin{aligned}
& + 2d_0 \text{Tr}(\bar{B}B) \text{Tr}((v \cdot a)^2) + 2d_1 \text{Tr}(\bar{B}v \cdot a) \text{Tr}(v \cdot aB) \\
& + 2d_K \text{Tr}(\bar{B}B) \left(v_\mu \text{Tr}[\partial^\mu U \cdot U^\dagger] \right)^2
\end{aligned}$$

where $v_\mu = (1; \vec{0})$ is a four-velocity. (We refer to [38, 39] for reviews of heavy-baryon theory.) Note the new $U_A(1)$ term proportional to d_K . Motivated by the lack of any kinetic term for Q in the meson Lagrangian (10) we do not include a term proportional to $(v_\mu \partial^\mu Q)^2$ although the $U_A(1)$ term d_K is understood to contain possible OZI violation.

The parameters b_D and b_F are determined from the baryon mass shifts: one finds [29] $b_D = +0.066 \text{GeV}^{-1}$ and $b_F = -0.213 \text{GeV}^{-1}$. The value of M_0 in Eq.(19) is fixed by the size of b_0 which is constrained by the size of the pion-nucleon sigma term. The five d_i parameters are fit to scattering data as done in Refs. [29, 31].

When we eliminate Q through its equation of motion the Q dependent terms in the effective Lagrangian become:

$$\begin{aligned}
\mathcal{L}_Q = & \frac{1}{12} \tilde{m}_{\eta_0}^2 \left[-6\eta_0^2 - \frac{\sqrt{6}}{M_0} \mathcal{G}_{QNN} F_0 \partial^\mu \eta_0 \text{Tr}(\bar{B} \gamma_\mu \gamma_5 B) \right. \\
& + \mathcal{G}_{QNN}^2 F_0^2 \left(\text{Tr} \bar{B} \gamma_5 B \right)^2 + 2 \mathcal{C} \frac{\tilde{m}_{\eta_0}^2}{F_0^2} \eta_0^2 \text{Tr}(\bar{B}B) \\
& \left. - \frac{\sqrt{6}}{3M_0 F_0} \mathcal{G}_{QNN} \mathcal{C} \tilde{m}_{\eta_0}^2 \eta_0 \partial^\mu \text{Tr}(\bar{B} \gamma_\mu \gamma_5 B) \text{Tr}(\bar{B}B) + \dots \right]
\end{aligned} \tag{26}$$

The third, fourth and fifth terms in the Lagrangian (26) are contact terms associated with the gluonic potential in Q . The last term in Eq.(26) is the gluonic contact term (3) in the low-energy $pp \rightarrow pp\eta'$ reaction with $g_{QNN} \equiv \sqrt{\frac{1}{6}} \mathcal{G}_{QNN} F_0 \tilde{m}_{\eta_0}^2$. The term

$$\mathcal{L}_{\text{contact}}^{(3)} = \frac{1}{6F_0^2} \mathcal{C} \tilde{m}_{\eta_0}^4 \eta_0^2 \text{Tr}(\bar{B}B). \tag{27}$$

is potentially important to η -nucleon and η' -nucleon scattering processes. It will contribute to the intermediate state in our coupled channels calculation as an *attractive* potential (6) in the Lippmann-Schwinger equation (4) for *positive* \mathcal{C} .

The OZI violating Lagrangian \mathcal{L}_Q is proportional to $\tilde{m}_{\eta_0}^2$ which vanishes in the formal OZI limit. Phenomenologically, the large masses of the η and η' mesons imply that there is no reason, a priori, to expect \mathcal{L}_Q to be small. We note that large N_c predictions for the η' -nucleon system should be treated with care. Assuming a continuous large N_c limit, one finds $m_{\eta'}^2 \sim 1/N_c$ and $M_N \sim N_c$ whereas $m_{\eta'}$ is greater than M_N in the real world! The large N_c approximation is badly violated in the $U_A(1)$ channel.

Some hint on the possible size of the $U_A(1)$ parameters in the chiral Lagrangian comes from the flavour-singlet Goldberger-Treiman relation (1). If OZI were exact in the singlet 1^+ channel the Ellis-Jaffe sum-rule would hold and one would find $g_A^{(0)} = g_A^{(8)} \simeq 0.6$. If one attributes the OZI suppression of the flavour-singlet axial-charge extracted from polarised deep inelastic scattering, $g_A^{(0)}|_{\text{pDIS}} = 0.2 - 0.35$, to the gluonic coupling g_{QNN} then one finds $g_{QNN} \sim 2.45$ or $\mathcal{G}_{QNN} \simeq +60 \text{GeV}^{-3}$. If one

further takes this value and saturates the COSY measurement [28] of the low-energy $pp \rightarrow pp\eta'$ cross-section with the contact term (3) then one finds $|\mathcal{C}| \simeq 2\text{GeV}^{-3}$ [17]. Of course, in practice, other processes will contribute to the measured $pp \rightarrow pp\eta'$ cross-section. However, this simple estimate does provide a handle on the possible size of the OZI violation parametrised by \mathcal{C} .

4 Results

To investigate the effect of OZI violation in the flavour-singlet $J^P = 1^+$ channel on the η and η' photoproduction processes we work with the Lippmann-Schwinger equation (4). The potentials for SU(3) (sub-)processes are listed in [29]. We have generalised these potentials to include η - η' mixing and the coupling of $U_A(1)$ degrees of freedom to the nucleon. The results are listed in the Appendix.

Our aim here is to investigate the qualitative effect of different possible OZI violations on the η and η' photoproduction cross-sections rather than to make quantitative predictions for η' scattering and production processes. We look for definite general effects in the cross-sections as we vary the OZI parameters.¹ We isolate which channels are the most important and check the consistency of our results by observing that they also hold when we decrease each of the meson masses by a uniform scaling factor $\lambda \simeq 0.75$ with the b_i and d_i held fixed.

The potentials have the following general features. Starting with $F_0 = F_\pi$ and $\mathcal{C} = d_K = 0$ the $U_A(1)$ potentials $C_{\eta\eta}$ and $C_{\eta'\eta'}$ are repulsive, and $C_{\eta\eta'}$ is attractive. For $\mathcal{C} = d_K = 0$ clearly the most prominent effect in these three potentials comes from the heavy-baryon terms (25); they contribute $+1.1E_\eta^2$ in $C_{\eta\eta}$, $-0.4E_\eta E_{\eta'}$ in $C_{\eta\eta'}$, and $+1.1E_{\eta'}^2$ in $C_{\eta'\eta'}$. The Born term contributions to the meson-baryon scattering potentials turn out to be very small. One finds a strong attractive coupling, $-1.1E_K E_{\eta'}$, of the $|\eta'N\rangle$ to $|K\Sigma\rangle^{(1/2)}$ states. Each of these $|\eta N\rangle$, $|\eta'N\rangle$ and $|K\Sigma\rangle^{(1/2)}$ intermediate states play an important role in generating the $\gamma p \rightarrow \eta' p$ cross-section.

In Fig 2 we show a fit to the η photoproduction cross-section from our S-wave calculation with η - η' mixing included and the OZI violating couplings and d_K turned off. We also show the S-wave contribution to the η' photoproduction cross-section which is generated with the same set of b_0 and d_i parameters. All figures are calculated with $\alpha_{\eta'N} = 1.5\text{GeV}$. The S-wave indeed dominates η photoproduction close to threshold through the $S_{11}(1535)$. This is not so for η' photoproduction where S-waves are expected to account only for part of the η' cross-section even close to threshold. The general results presented below do not depend strongly on $\alpha_{\eta'N}$, for $\alpha_{\eta'N}$ between 1 and 2GeV. Figs. 2-6 are calculated with the flavour-singlet coupling $g_{\eta_0 NN}$ set equal to its OZI value, corresponding to $X = 0.58$ in Eq.(30) below. Approximately, the η' photoproduction cross-section grows proportional to the singlet

¹ Several caveats are in order if one wishes to extend the analysis presented here from a qualitative to a quantitative description and to make numerical predictions for η' production using this type of approach – two of them associated with the large η' mass. First, the potentials in [29] are derived assuming $E_i \ll M_0$ for meson energies, which may provide a reasonable approximation for the η but not for physical η' photoproduction. For the physical η' mass we are close to the limit of valid application of the effective theory, $\mu \sim 4\pi F_\pi$.

coupling $g_{\eta_0 NN}$ and the η photoproduction cross-section is independent of $g_{\eta_0 NN}$

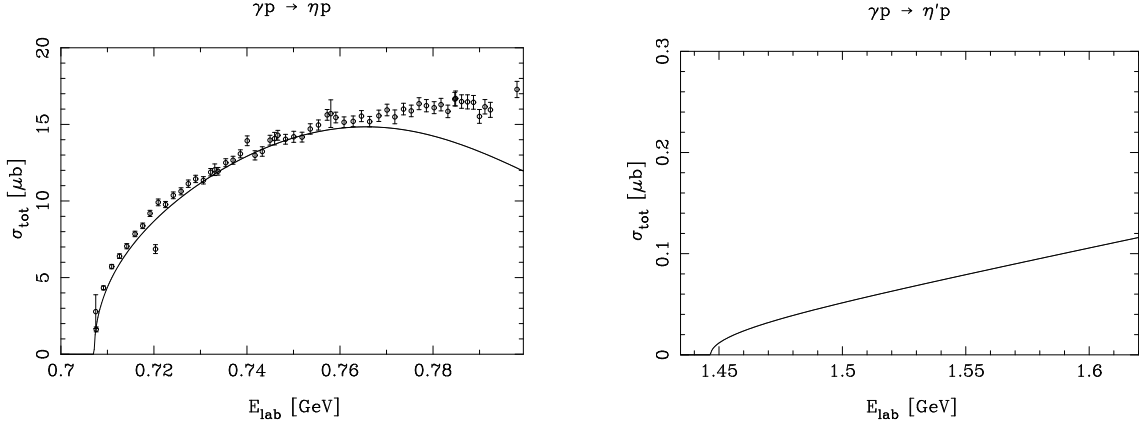


Figure 2: *Fit to the low-energy η photoproduction data [12] with $\mathcal{C} = d_K = 0$, and the η' photoproduction cross-section generated from the same fit parameters*

For positive \mathcal{C} the gluonic term (27) is attractive in each of the $C_{\eta\eta}$, $C_{\eta\eta'}$ and $C_{\eta'\eta'}$ potentials. Motivated by the COSY measurement of $pp \rightarrow pp\eta'$ close to threshold we vary \mathcal{C} from -4 to $+4\text{GeV}^{-3}$, which we consider a reasonable guess at its maximum likely magnitude. With increasing positive \mathcal{C} in our “reasonable range” the η and η' cross-sections are enhanced very close to threshold and the broad maximum in the η production cross-section shifts closer to threshold. With increasing negative \mathcal{C} they are suppressed and the peak in the η production cross-section shifted to higher energy. We show this in Fig.3 keeping the b_0 and d_i parameters fixed at their OZI values for $\mathcal{C} = 0, \pm 2$. It is not unreasonable that a large gluonic production mechanism in the low-energy $pp \rightarrow pp\eta'$ reaction and the shape of the $S_{11}(1535)$ resonance may be correlated.

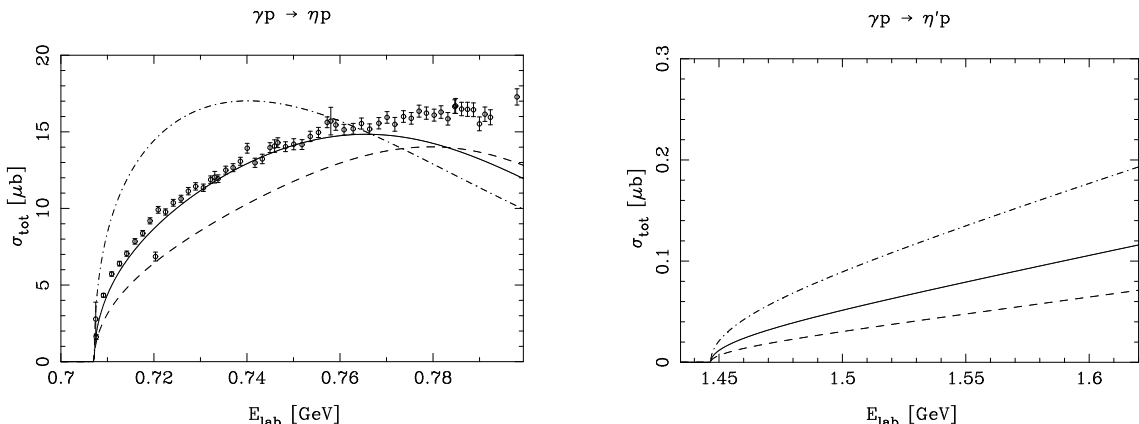


Figure 3: *The fit from Fig. (2), solid line, together with the η and η' photoproduction cross-sections produced by varying the gluonic coupling $\mathcal{C} = +2$, dot-dashed line, and $\mathcal{C} = -2$, dashed line, with all other parameters held fixed.*

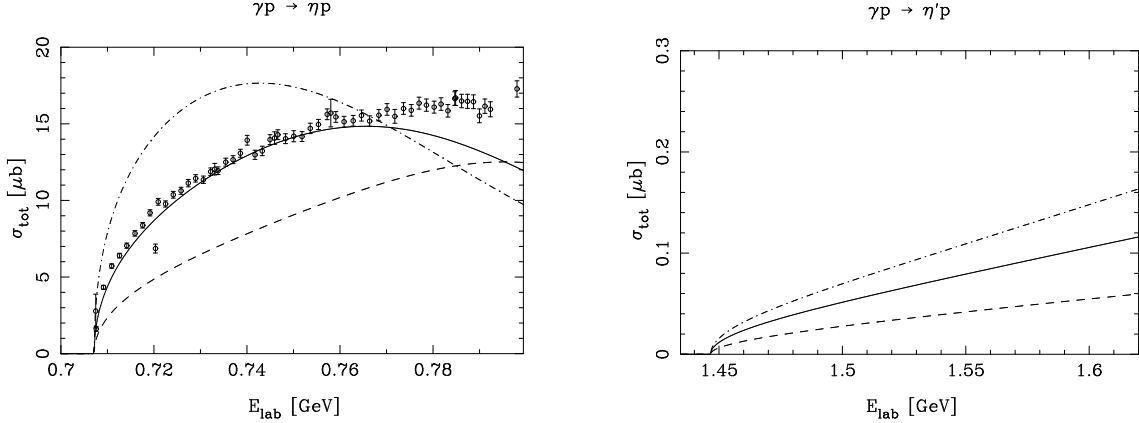


Figure 4: The fit from Fig. (2), solid line, together with the η and η' photoproduction cross-sections produced by varying $\frac{F_\pi}{F_0} = 0.8$, dot-dashed line, and $\frac{F_\pi}{F_0} = 1.25$, dashed line, with all other parameters held fixed.

Varying F_π/F_0 between 0.8 and 1.25 we find that the photoproduction cross-sections are enhanced close to threshold for larger values of F_0 – see Fig. 4, corresponding to an enhanced heavy-baryon repulsion in $C_{\eta'\eta'}$.

We also consider the effect of the heavy-baryon term proportional to d_K in Eq.(25). We find that the η' photoproduction cross-section is enhanced for values of d_K in a small window around -0.035. We show this in Fig.5.

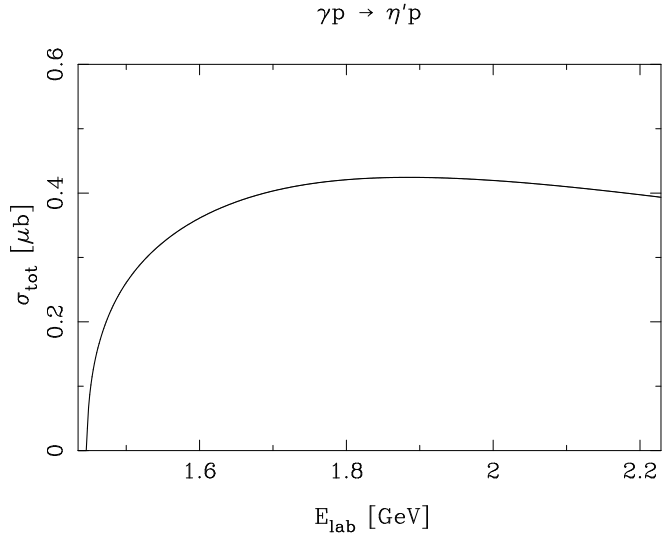


Figure 5: The η' photoproduction cross-section is enhanced with a small negative $d_K = -0.035$. Here $\mathcal{C} = 0$ and $F_0 = F_\pi$.

Finally, we consider the effect of varying the gluonic contribution to the singlet mass: $\tilde{m}_{\eta_0}^2$. Varying the $\tilde{m}_{\eta_0}^2$ means varying the masses of both the η and η' mesons which, in turn, means varying the $\eta-\eta'$ mixing angle θ . Setting $F_0 = F_\pi$ one may diagonalise the $\eta-\eta'$ mass matrix which follows from (15) to obtain the masses of

the physical η and η' mesons:

$$m_{\eta',\eta}^2 = (m_K^2 + \tilde{m}_{\eta_0}^2/2) \pm \frac{1}{2} \sqrt{(2m_K^2 - 2m_\pi^2 - \frac{1}{3}\tilde{m}_{\eta_0}^2)^2 + \frac{8}{9}\tilde{m}_{\eta_0}^4}. \quad (28)$$

If we turn off the gluon mixing term, then one finds $m_{\eta'} = \sqrt{2m_K^2 - m_\pi^2}$ and $m_\eta = m_\pi$. Summing over the two eigenvalues yields [15]

$$m_\eta^2 + m_{\eta'}^2 = 2m_K^2 + \tilde{m}_{\eta_0}^2. \quad (29)$$

Substituting the physical values of $(m_\eta^2 + m_{\eta'}^2)$ in Eq.(29) and m_K^2 yields $\tilde{m}_{\eta_0}^2 = 0.73\text{GeV}^2$, which corresponds to $m_\eta = 499\text{MeV}$ and $m_{\eta'} = 984\text{MeV}$. The value $\tilde{m}_{\eta_0}^2 = 0.73\text{GeV}^2$ corresponds to an $\eta - \eta'$ mixing angle $\theta \simeq -18$ degrees – the physical value. As we decrease $\tilde{m}_{\eta_0}^2$ the $S_{11}(1535)$ peak in the η photoproduction cross-section splits into two resonance-like structures – Fig.6. The heavier structure is associated with a $K\Sigma$ quasi-bound state; the second, close to threshold, involves strong coupling to the $K\Lambda$ and ηN channels through the $K\Lambda \leftrightarrow \eta N$ potential.

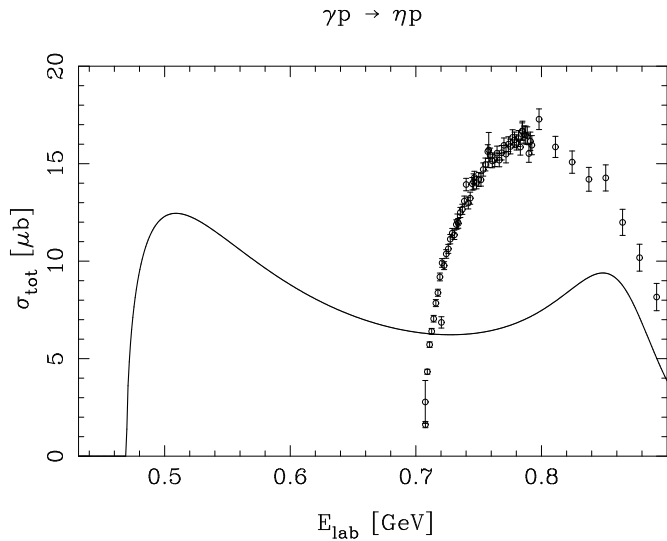


Figure 6: Reducing the gluonic contribution to the η and η' masses by changing $\tilde{m}_{\eta_0}^2$ from 0.73 to 0.25 GeV^2 , the η and η' masses in (28) become 0.15 GeV and 0.59 GeV respectively and the $S_{11}(1535)$ splits into two resonance-like structures.

5 Conclusions

Gluon dynamics through OZI violation play a potentially important role in the η and η' nucleon interactions. Through the axial anomaly gluonic degrees of freedom generate about $300 - 400$ MeV of the η and η' masses, and thereby affect the threshold behaviour of η and η' photo- and proton-induced production. They also induce new gluonic coupling constants in the η and η' nucleon interactions. Our coupled channels analysis hints at a strong correlation between the gluonic contribution to

the low-energy $pp \rightarrow pp\eta'$ reaction and the sharp rise of the $\gamma p \rightarrow \eta p$ cross-section close to threshold. It follows that gluonic effects in the axial U(1) channel may be important in the structure of the $N^*(1535)$ resonance which couples strongly to the η . The S-wave contribution to the η' photoproduction cross-section close to threshold also increases with increasing positive gluonic coupling \mathcal{C} . For η' photoproduction higher partial waves are likely to be important in building up the total η' photoproduction cross-section.

Acknowledgements

SDB thanks for the European Centre ECT*, Trento for a Senior Visiting Fellowship where part of this work was completed. We thank B. Borasoy and N. Kaiser for helpful discussions. We also thank J. Link and B. Ritchie for communication about present and forthcoming experiments.

References

- [1] G. Veneziano, Okubofest lecture, CERN preprint TH-5840 (1990).
- [2] G.M. Shore, Zuoz lecture, hep-ph/9812354.
- [3] S. Weinberg, Phys. Rev. **D11** (1975) 3583.
- [4] G. Christos, Phys. Rept. **116** (1984) 251.
- [5] G. 't Hooft, Phys. Rev. Lett. **37** (1976) 8; Phys. Rev. **D14** (1976) 3432.
- [6] H. Fritzsch and P. Minkowski, Nuovo Cimento **30A** (1975) 393.
- [7] G. Veneziano, Nucl. Phys. **B159** (1979) 213; Phys. Lett. **B95** (1980) 90.
- [8] E. Witten, Nucl. Phys. **B156** (1979) 269.
- [9] S.L. Adler, Phys. Rev. **177** (1969) 2426.
- [10] J.S. Bell and R. Jackiw, Nuovo Cimento **60A** (1969) 47.
- [11] S. Okubo, Phys. Lett. **5** (1963) 165;
G. Zweig, CERN report No. 8419/TH412 (1964);
J. Iizuka, Prog. Theor. Phys. Suppl. **37-38** (1966) 21.
- [12] The TAPS Collaboration, (B. Krusche et al.), Phys. Rev. Lett. **77** (1995) 3736.
- [13] The SAPHIR Collaboration, (R. Plötzke et al.), Phys. Lett. **B444** (1998) 555.
- [14] CEBAF experiments E-91-008 and E-94-008 (B.G. Ritchie et al.);
B. Ritchie, in Proc. Int. Workshop on *The Structure of the η' Meson* eds. M. Burkardt et al. (World Scientific 1997).
- [15] P. Di Vecchia and G. Veneziano, Nucl. Phys. **B171** (1980) 253.
- [16] C. Rosenzweig, J. Schechter and C.G. Trahern, Phys. Rev. **D21** (1980) 3388;
P. Nath and R. Arnowitt, Phys. Rev. **D23** (1981) 473.
- [17] S. D. Bass, hep-ph/9907373, Phys. Lett **B463** (1999) 286; hep-ph/0006348.
- [18] G. Veneziano, Mod. Phys. Lett. **A4** (1989) 1605;
G.M. Shore and G. Veneziano, Nucl. Phys. **B381** (1992) 23.
- [19] T. Hatsuda, Nucl. Phys. **B329** (1990) 376.
- [20] S. D. Bass, hep-ph/9902280, Eur. Phys. J **A5** (1999) 17.
- [21] R. Windmolders, hep-ph/9905505.
- [22] B. Lampe and E. Reya, Phys. Rept. **332** (2000) 1.
- [23] R. Machleidt, K. Holinde and Ch. Elster, Phys. Rept. **149** (1987) 1.

- [24] J-F. Germond and C. Wilkin, Nucl. Phys. **A518** (1990) 308.
- [25] G. Fäldt and C. Wilkin, Z Physik **A357** (1997) 241.
- [26] SATURNE, F. Hibou et al., Phys. Lett. **B438** (1998) 41.
- [27] The CELSIUS Collaboration (H. Calen et al.), Phys. Rev. Lett. **80** (1998) 2069; Phys. Rev. **C58** (1998) 2667.
- [28] The COSY-11 Collaboration (P. Moskal et al.), Phys. Rev. Lett. **80** (1998) 3202; Phys. Lett. **B474** (2000) 416.
- [29] N. Kaiser, T. Waas and W. Weise, Nucl. Phys. **A612** (1997) 297.
- [30] N. Kaiser, P.B. Siegel and W. Weise, Nucl. Phys. **A594** (1995) 325; Phys. Lett. **B362** (1995) 23.
- [31] J. Caro Ramon, N. Kaiser, S. Wetzel and W. Weise, Nucl. Phys. **A672** (2000) 249.
- [32] S.L. Adler and W.A. Bardeen, Phys. Rev. **182** (1969) 1517.
- [33] F.J. Gilman and R. Kauffman, Phys. Rev. **D36** (1987) 2761; (E) **D37** (1988) 3348.
- [34] P. Ball, J.M. Frere and M. Tytgat, Phys. Lett. **B365** (1996) 367.
- [35] G. M. Shore and G. Veneziano, Nucl. Phys. **B381** (1992) 3; G. M. Shore, Nucl. Phys. **B569** (2000) 107.
- [36] The Particle Data Group, C. Caso et al., Eur. Phys. J **C3** (1998) 1.
- [37] F.E. Close and R.G. Roberts, Phys. Lett. **B316** (1993) 165.
- [38] E. Jenkins and A.V. Manohar, ECSD/PTH 91-30.
- [39] V. Bernard, N. Kaiser and U. Meissner, Int. J. Mod. Phys. **E4** (1995) 193.
- [40] J. Ellis and R.L. Jaffe, Phys. Rev. **D9** (1974) 1444; (E) **D10** (1974) 1669.

Appendix: Potentials for the $U_A(1)$ sector

The S-wave potential for photoproduction

To simplify the notation we define

$$X = \left(2D + 2K + \mathcal{G}_{QNN} F_0^2 \frac{\tilde{m}_{\eta_0}^2}{2M_0} \right) \quad (30)$$

The S-wave potentials for photoproduction become

$$B_{0+}^{(2)} = \frac{eM_N}{8\pi F_\pi \sqrt{3s}} (3F - D) \left[\cos \theta Y_\eta + \sin \theta Y_{\eta'} \right] \quad (31)$$

and

$$B_{0+}^{(5)} = \frac{eM_N}{8\pi F_\pi \sqrt{3s}} \frac{F_\pi}{F_0} X \left[\cos \theta Y_{\eta'} - \sin \theta Y_\eta \right] \quad (32)$$

where

$$Y_\phi = -\frac{1}{3M_0} \left(2E_\phi + \frac{m_\phi^2}{E_\phi} \right) \quad (33)$$

In Eqs.(31) and (32) Y_η corresponds to η photoproduction and $Y_{\eta'}$ corresponds to η' photoproduction.

S-wave potentials for meson-baryon scattering

Following [29] we define

$$S_{ab} = \frac{E_a E_b}{2M_0} \quad (34)$$

$$U_{ab} = \frac{1}{3M_0} \left(2m_a^2 + 2m_b^2 + \frac{m_a^2 m_b^2}{E_a E_b} - \frac{7}{2} E_a E_b \right) \quad (35)$$

Potentials with η and η'

Working with the notation of Eq.(5) one finds:

$$\begin{aligned} C_{1\eta} &= \frac{1}{4} (F + D) \left(\cos \theta (3F - D) - \sqrt{2} \sin \theta X \frac{F_\pi}{F_0} \right) \left(S_{\pi\eta} + U_{\pi\eta} \right) \\ &\quad - (d_D + d_F) \left(\cos \theta - \sqrt{2} \sin \theta \frac{F_\pi}{F_0} \right) E_\pi E_\eta \\ &\quad + m_\pi^2 (b_D + b_F) \left[2 \cos \theta - 2\sqrt{2} \sin \theta \frac{F_\pi}{F_0} \right] \end{aligned} \quad (36)$$

$$\begin{aligned} C_{1\eta'} &= \frac{1}{4} (F + D) \left(\sin \theta (3F - D) + \sqrt{2} \cos \theta X \frac{F_\pi}{F_0} \right) \left(S_{\pi\eta'} + U_{\pi\eta'} \right) \\ &\quad - (d_D + d_F) \left(\sin \theta + \sqrt{2} \cos \theta \frac{F_\pi}{F_0} \right) E_\pi E_{\eta'} \\ &\quad + m_\pi^2 (b_D + b_F) \left[2 \sin \theta + 2\sqrt{2} \cos \theta \frac{F_\pi}{F_0} \right] \end{aligned} \quad (37)$$

$$\begin{aligned}
C_{\eta 3} = & \left[\left(\frac{1}{12} D^2 - \frac{3}{4} F^2 \right) \cos \theta + \frac{\sqrt{2}}{12} (3F + D) \sin \theta X \frac{F_\pi}{F_0} \right] S_{K\eta} \quad (38) \\
& + \left[\frac{1}{2} D(F + \frac{1}{3}D) \cos \theta + \frac{\sqrt{2}}{12} (3F + D) \sin \theta X \frac{F_\pi}{F_0} \right] U_{K\eta} \\
& - \left[\left(\frac{1}{6} d_D + \frac{1}{2} d_F + d_1 \right) \cos \theta + \frac{\sqrt{2}}{3} (d_D + 3d_F) \sin \theta \frac{F_\pi}{F_0} \right] E_K E_\eta \\
& + (b_D + 3b_F) \left[\left(\frac{5}{6} m_K^2 - \frac{1}{2} m_\pi^2 \right) \cos \theta + \frac{2}{3} \sqrt{2} m_K^2 \sin \theta \frac{F_\pi}{F_0} \right] \\
& + \frac{3}{8} (E_K + \cos \theta E_\eta) + \frac{3}{16 M_0} \left[E_K^2 - m_K^2 + \cos \theta (E_\eta^2 - m_\eta^2) \right]
\end{aligned}$$

$$\begin{aligned}
C_{\eta' 3} = & \left[\left(\frac{1}{12} D^2 - \frac{3}{4} F^2 \right) \sin \theta - \frac{\sqrt{2}}{12} (3F + D) \cos \theta X \frac{F_\pi}{F_0} \right] S_{K\eta} \quad (39) \\
& + \left[\frac{1}{2} D(F + \frac{1}{3}D) \sin \theta - \frac{\sqrt{2}}{12} (3F + D) \cos \theta X \frac{F_\pi}{F_0} \right] U_{K\eta} \\
& - \left[\left(\frac{1}{6} d_D + \frac{1}{2} d_F + d_1 \right) \sin \theta - \frac{\sqrt{2}}{3} (d_D + 3d_F) \cos \theta \frac{F_\pi}{F_0} \right] E_K E_{\eta'} \\
& + (b_D + 3b_F) \left[\left(\frac{5}{6} m_K^2 - \frac{1}{2} m_\pi^2 \right) \sin \theta - \frac{2}{3} \sqrt{2} m_K^2 \cos \theta \frac{F_\pi}{F_0} \right] \\
& + \frac{3}{8} (E_K + \sin \theta E_{\eta'}) + \frac{3}{16 M_0} \left[E_K^2 - m_K^2 + \sin \theta (E_{\eta'}^2 - m_{\eta'}^2) \right]
\end{aligned}$$

$$\begin{aligned}
C_{\eta 4} = & \left[\frac{1}{4} (3F - D)(D - F) \cos \theta - \frac{1}{2\sqrt{2}} (D - F) \sin \theta X \frac{F_\pi}{F_0} \right] S_{K\eta} \quad (40) \\
& + \left[\frac{1}{2} D(D - F) \cos \theta - \frac{1}{2\sqrt{2}} (D - F) \sin \theta X \frac{F_\pi}{F_0} \right] U_{K\eta} \\
& + (d_D - d_F) \left[\frac{1}{2} \cos \theta + \sqrt{2} \sin \theta \frac{F_\pi}{F_0} \right] E_K E_\eta \\
& + (b_D - b_F) \left[\left(\frac{3}{2} m_\pi^2 - \frac{5}{2} m_K^2 \right) \cos \theta - 2\sqrt{2} m_K^2 \sin \theta \frac{F_\pi}{F_0} \right] \\
& + \frac{3}{8} (E_K + \cos \theta E_\eta) + \frac{3}{16 M_0} \left[E_K^2 - m_K^2 + \cos \theta (E_\eta^2 - m_\eta^2) \right]
\end{aligned}$$

$$\begin{aligned}
C_{\eta' 4} = & \left[\frac{1}{4} (3F - D)(D - F) \sin \theta + \frac{1}{2\sqrt{2}} (D - F) \cos \theta X \frac{F_\pi}{F_0} \right] S_{K\eta} \quad (41) \\
& + \left[\frac{1}{2} D(D - F) \sin \theta + \frac{1}{2\sqrt{2}} (D - F) \cos \theta X \frac{F_\pi}{F_0} \right] U_{K\eta} \\
& + (d_D - d_F) \left[\frac{1}{2} \sin \theta - \sqrt{2} \cos \theta \frac{F_\pi}{F_0} \right] E_K E_{\eta'}
\end{aligned}$$

$$\begin{aligned}
& + (b_D - b_F) \left[\left(\frac{3}{2} m_\pi^2 - \frac{5}{2} m_K^2 \right) \sin \theta + 2\sqrt{2} m_K^2 \cos \theta \frac{F_\pi}{F_0} \right] \\
& + \frac{3}{8} (E_K + \sin \theta E_{\eta'}) + \frac{3}{16 M_0} \left[E_K^2 - m_K^2 + \sin \theta (E_{\eta'}^2 - m_{\eta'}^2) \right]
\end{aligned}$$

$$\begin{aligned}
C_{\eta\eta} &= \left[\frac{1}{12} (3F - D)^2 \cos^2 \theta - \frac{\sqrt{2}}{24} (3F - D) X \frac{F_\pi}{F_0} \sin 2\theta \right. \\
&\quad \left. + \frac{1}{6} X^2 \left(\frac{F_\pi}{F_0} \right)^2 \sin^2 \theta \right] (S_{\eta\eta} + U_{\eta\eta}) \\
&\quad - \frac{1}{3} \mathcal{C} \tilde{m}^4 \left(\frac{F_\pi}{F_0} \right)^2 \sin^2 \theta \\
&\quad + \left[\left(d_F - \frac{5}{3} d_D - 2d_0 \right) \cos^2 \theta - \frac{\sqrt{2}}{2} \left(\frac{d_D}{3} - d_F \right) \frac{F_\pi}{F_0} \sin 2\theta \right. \\
&\quad \left. + \left(-2d_0 - \frac{4}{3} d_D + 24d_K \right) \left(\frac{F_\pi}{F_0} \right)^2 \sin^2 \theta \right] E_\eta E_\eta \\
&\quad + \left[\frac{16}{3} m_K^2 (b_D - b_F + b_0) + 2m_\pi^2 \left(\frac{5}{3} b_F - b_D - \frac{2}{3} b_0 \right) \right] \cos^2 \theta \\
&\quad - \frac{1}{2} \left[\frac{\sqrt{2}}{2} m_\pi^2 (3b_D - b_F + 4b_0) + 2\sqrt{2} m_K^2 (-b_D + b_F - b_0) \right] \frac{F_\pi}{F_0} \sin 2\theta \\
&\quad + \frac{4}{3} \left[m_\pi^2 (2b_F + b_0) + 2m_K^2 (b_D - b_F + b_0) \right] \left(\frac{F_\pi}{F_0} \right)^2 \sin^2 \theta
\end{aligned} \tag{42}$$

$$\begin{aligned}
C_{\eta\eta'} &= \left[\frac{1}{24} (3F - D)^2 \sin 2\theta - \frac{\sqrt{2}}{12} (3F - D) X \frac{F_\pi}{F_0} \cos 2\theta \right. \\
&\quad \left. - \frac{1}{12} X^2 \left(\frac{F_\pi}{F_0} \right)^2 \sin 2\theta \right] (S_{\eta\eta'} + U_{\eta\eta'}) \\
&\quad + \frac{1}{6} \mathcal{C} \tilde{m}^4 \left(\frac{F_\pi}{F_0} \right)^2 \sin 2\theta \\
&\quad + \left[\frac{1}{2} \left(d_F - \frac{5}{3} d_D - 2d_0 \right) \sin 2\theta - \sqrt{2} \left(\frac{d_D}{3} - d_F \right) \frac{F_\pi}{F_0} \cos 2\theta \right. \\
&\quad \left. - \frac{1}{2} \left(-2d_0 - \frac{4}{3} d_D + 24d_K \right) \left(\frac{F_\pi}{F_0} \right)^2 \sin 2\theta \right] E_\eta E_{\eta'} \\
&\quad + \frac{1}{2} \left[\frac{16}{3} m_K^2 (b_D - b_F + b_0) + 2m_\pi^2 \left(\frac{5}{3} b_F - b_D - \frac{2}{3} b_0 \right) \right] \sin 2\theta \\
&\quad - \left[\frac{\sqrt{2}}{2} m_\pi^2 (3b_D - b_F + 4b_0) + 2\sqrt{2} m_K^2 (-b_D + b_F - b_0) \right] \frac{F_\pi}{F_0} \cos 2\theta \\
&\quad - \frac{2}{3} \left[m_\pi^2 (2b_F + b_0) + 2m_K^2 (b_D - b_F + b_0) \right] \left(\frac{F_\pi}{F_0} \right)^2 \sin 2\theta
\end{aligned} \tag{43}$$

$$C_{\eta'\eta'} = \left[\frac{1}{12} (3F - D)^2 \sin^2 \theta + \frac{\sqrt{2}}{24} (3F - D) X \frac{F_\pi}{F_0} \sin 2\theta \right] \tag{44}$$

$$\begin{aligned}
& + \frac{1}{6} X^2 \left(\frac{F_\pi}{F_0} \right)^2 \cos^2 \theta \left[\left(S_{\eta' \eta'} + U_{\eta' \eta'} \right) \right. \\
& - \frac{1}{3} \mathcal{C} \tilde{m}^4 \left(\frac{F_\pi}{F_0} \right)^2 \cos^2 \theta \\
& + \left[\left(d_F - \frac{5}{3} d_D - 2d_0 \right) \sin^2 \theta + \frac{\sqrt{2}}{2} \left(\frac{d_D}{3} - d_F \right) \frac{F_\pi}{F_0} \sin 2\theta \right. \\
& \quad \left. + \left(-2d_0 - \frac{4}{3} d_D + 24d_K \right) \left(\frac{F_\pi}{F_0} \right)^2 \cos^2 \theta \right] E_{\eta'} E_{\eta'} \\
& + \left[\frac{16}{3} m_K^2 (b_D - b_F + b_0) + 2m_\pi^2 \left(\frac{5}{3} b_F - b_D - \frac{2}{3} b_0 \right) \right] \sin^2 \theta \\
& + \frac{1}{2} \left[\frac{\sqrt{2}}{2} m_\pi^2 (3b_D - b_F + 4b_0) + 2\sqrt{2} m_K^2 (-b_D + b_F - b_0) \right] \frac{F_\pi}{F_0} \sin 2\theta \\
& + \frac{4}{3} \left[m_\pi^2 (2b_F + b_0) + 2m_K^2 (b_D - b_F + b_0) \right] \left(\frac{F_\pi}{F_0} \right)^2 \cos^2 \theta
\end{aligned}$$